J Therm Anal Calorim (2012) 109:855–861
DOI 10.1007/s10973-011-1858-1

Synthesis, characterization, and thermochemistry of acid attack of "B" type carbonate fluorapatites

Houda Zendah · Ismail Khattech · Mohamed Jemal

Received: 15 April 2011 / Accepted: 10 August 2011 / Published online: 9 September 2011

Abstract A series of "B" type carbonate fluorapatites (B–CO_3–Fap) have been synthesized and characterized by X-ray diffraction, infrared spectroscopy, and chemical analysis. The thermochemical study of phosphoric acid attack of the products was performed by a 19% w/w P_2O_5 solution on raw and deconvoluted curves. The calculated thermogenesis curves show one, two, or four peaks, depending on the mass of dissolved solid and the carbonate content in B–CO_3–Fap. The plot of the quantity of heat measured by integrating the raw signal as a function of the dissolved mass in the same volume solution presents three straight segments for low-carbonated and two segments for moderately carbonated ones. From the slopes of line segments, it was possible to determine the enthalpies of dissolution of "B" type carbonate fluorapatites and to deduce that of precipitation of CaF_2 and $Ca(H_2PO_4)_2{\cdot}H_2O$, which have been compared to directly measured or literature data.

Keywords Carbonate fluorapatites · Microcalorimetry · Dissolution · Deconvolution

Introduction

Apatites are crystalline solids isomorphic of fluorapatite phosphate (CaFap), $Ca_{10}(PO_4)F_2$. The latter is considered as a reference compound because it exists at almost pure natural state and is the most stable in the family of apatites. The structure of the CaFap was determined for the first time in 1930 by Naray and Mehnel [1, 2]. CaFap has an hexagonal structure with space group $P6_{3/m}$ [3]. Some substitutions of calcium, phosphate, or fluoride can occur. Among these substitutions, the partial replacement of the F^- and $PO_4{}^{3-}$ ions by the carbonate ions presents a special interest generated by the similarity of the carbonated compounds with the natural apatites. There are two possibilities of $CO_3{}^{2-}$ substitution leading to "A" type carbonate apatite, where the carbonate ions are replacing the fluoride ions located on the helical senary axis of the apatite lattice, or to "B" type carbonate fluorapatite, where the carbonate ions are located at the $PO_4{}^{3-}$ sites causing the creation of vacancies in the apatitic network [4, 5]. These two mechanisms can exist simultaneously. For the "B" type carbonate fluorapatites, the general formula is:

$$Ca_{10-x+u}(PO_4)_{6-x}(CO_3)_xF_{2-x+2u} \quad (1)$$

with the $0 < x < 2$ and "u" representing the number of fluoride ions associated with carbonate ions. The value of "u" factor depends on the composition of the medium in which the apatite was precipitated [6].

Consequently, physicochemical studies, especially by E.S.R. [6, 7] and thermogravimetric with simultaneous gas chromatography analyses [4, 8] suggested two modes for $CO_3{}^{2-}$ ions replacing $PO_4{}^{3-}$ ions. These are:

(i) ($CO_3{}^{2-}$, F^-) ion pairs replacing $PO_4{}^{3-}$. In accordance with this type of substitution, Vignoles et al. [7] proposed the structural formula as:

$$Ca_{10}(PO_4)_{6-x}(CO_3F)_x(F)_2 \quad (2)$$

(ii) $CO_3{}^{2-}$ ions replacing $PO_4{}^{3-}$ with the formation of adjacent F^- and Ca^{2+} vacancies ($CO_3{}^{2-}$, □). This mechanism is similar to the earlier proposal suggested by Labarthe et al. [9]. One or the other mechanism of substitution is preponderant depending on the ion

---

H. Zendah · I. Khattech (✉) · M. Jemal
Applied Thermodynamics Laboratory, Department
of Chemistry, Faculty of Science, Tunis-El Manar University,
2092 Tunis El Manar, Tunisia
e-mail: ismail.khattech@fst.rnu.tn

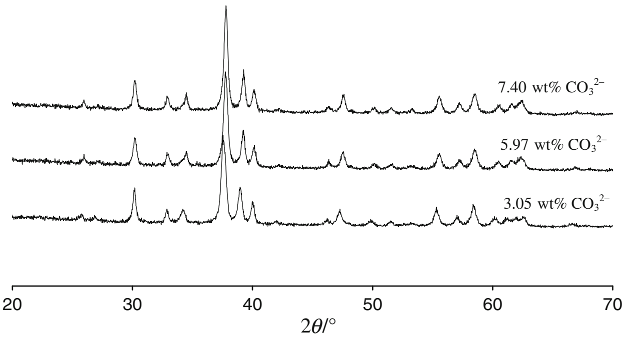

Fig. 1 Diffraction patterns of three B–CO_3–Fap samples

concentration in precipitation medium, that is “direct” or “reverse” precipitation method [7, 8] and so the general formula derived from (I) for “B” type carbonate apatites [7] can be expressed as:

$$Ca_{10-x+u}(PO_4)_{6-x}(CO_3)_{x-u}(CO_3F)_u(F)_{2-x+u} \tag{3}$$

A statistical study carried out by Bel Hadj Yahia and Jemal [10] has confirmed the presence of two types of substitution in the “B” type carbonate fluorapatites. According to these authors, the most probable substitutions in this kind of products are couple substitutions (CO_3^{2-}, F^-) for PO_4^{3-} and ($2CO_3^{2-}$, V^{ca}) for $2PO_4^{3-}$.

In a previous paper, performed on the thermochemical aspect of the dissolution of synthetic fluorapatites at various solid/liquid ratio, Brahim et al. [11] showed that at low values of that ratio only dissolution appeared, then increasing the ratio led to precipitation of monocalcium phosphate monohydrate ($Ca(H_2PO_4)_2 \cdot H_2O$), or to a mixture of the latter with dicalcium phosphate dihydrate ($CaHPO_4 \cdot 2H_2O$).

This study deals with the calorimetric analysis of the attack of “B” type carbonate fluorapatites with a phosphoric acid solution having a composition close to that used in industry (19% w/w P_2O_5). Calorimetry enables to follow in real time the attack reaction, and allows to understand the role of carbonates in the acid attack of phosphate rock. The recorded signals were processed according to the procedure developed by Brahim et al. [12] in order to get the deconvoluted curves showing the successive steps occurring in the process.

Synthesis and characterization of the apatites

A series of “B” type carbonate fluorapatites (B–CO_3–Fap) have been synthesized with different amount of carbonate, using the “reverse” procedure [6, 13]. This method consists in adding drop by drop a “B” solution containing ammonium phosphate (0.016 M), ammonium fluoride (0.04 M) and ammonium carbonate ($0.5 < [CO_3^{2-}]/[PO_4^{3-}] < 6$) in a boiling “A” solution containing the calcium nitrate (0.04 M). The pH of the precipitation medium was maintained between 8 and 9 by addition of ammonia (28% weight).

The purity of the products was checked by infrared spectroscopy, X-ray diffraction and chemical analysis.

X-ray analysis was performed using an X-ray diffractometer MRD with a generator (40 kV and 40 mA). The scanning speed is 0.04° 2θ/s. X-ray diffractograms show thin rays indicating that all the solids are formed of a well crystallized phase whatever the amount of carbonate introduced.

Figure 1 represents the X-ray diffractograms of three apatite samples. It shows characteristic peaks of apatite structure. The compounds crystallise in the hexagonal system, in the space group $P6_3/m$ [13]. The indexation of diffractogram in the hexagonal system was used to calculate the crystallographic parameters, with the “wincell” refinement program.

Table 1 gives the ‘*a*’ and ‘*c*’ parameters of various CO_3–Fap, preheated at 300 °C. For comparison, column 2 shows also the crystallographic parameters of the free carbonate phosphate fluorapatite together with the corresponding literature values.

IR spectra were recorded using a Perkin-Elmer 7700 FT–IR spectrometer between 400 and 4000 cm^{-1} in KBr pellets. They present only bands characterizing apatite specimens, Fig. 2. Bands at 1037, 1110, and 964 cm^{-1} are attributed to the vibrational modes of PO_4^{3-} groups [14, 15]. Bands at 565 and 706 cm^{-1} are assigned to P–O mode [16] and 469 cm^{-1} band results from the υ_2 phosphate mode [17]. In addition, the bands corresponding to CO_3^{2-} ions [18] appear at (876–1420–1463 cm^{-1}) and increase in intensity as CO_3^{2-} amount increases.

Table 1 “*a*” and “*c*” parameters of the Ca–Fap and the B–CO_3–Fap

$[CO_3^{2-}]/[PO_4^{3-}]$	$^{0/}$CaFap	0.5	1	2	3	4	5	6
a parameter/Å	9.372(3) 9.371[a]	9.355(3)	9.359(10)	9.333(9)	9.312(7)	9.300(10)	9.280(8)	9.289(8)
c parameter/Å	6.884(2) 6.890[a]	6.900(2)	6.911(6)	6.903(5)	6.903(4)	6.914(6)	6.928(5)	6.935(5)

[a] Literature values [14]

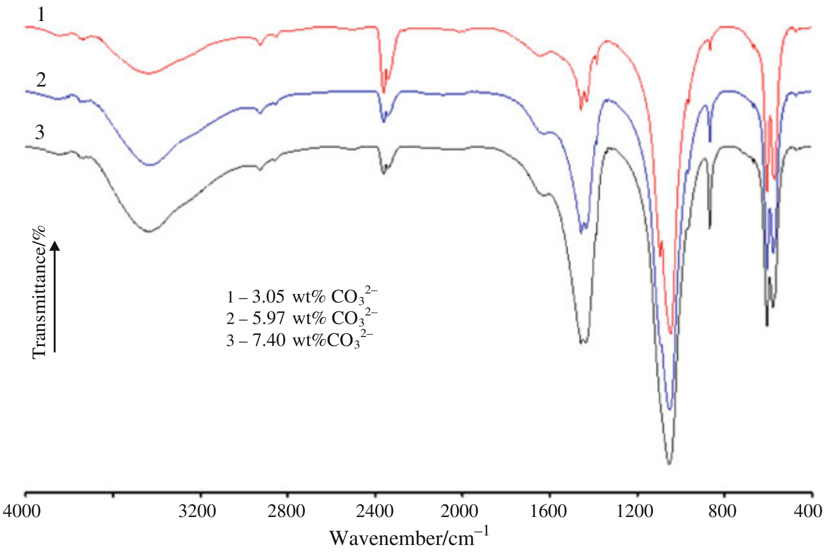

Fig. 2 Infrared spectra of three B–CO_3–Fap samples

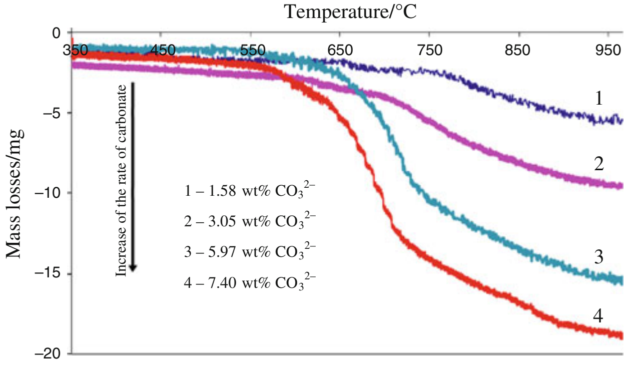

Fig. 3 Thermogravimetry curves of different carbonate apatites (Obtained under the same conditions)

The absence of bands between 600 and 1090 cm^{-1} shows that the products are free from HPO_4^{2-} ions. However, parasite bands appear at 3450, 2890, and 1400 cm^{-1}. They probably results from water retained by KBr.

The carbonate amount was determined by thermogravimetry, using a thermobalance (type B60, SETARAM, French). Carbonates decompose into carbon dioxide by heating the solids up to 1000 at 150 °C/h rate under inert gas flow (Argon). Preliminary experiments showed that CO_2 release finished at about 1000 °C [8]. Figure 3 shows the superposition of three thermogravimetry curves corresponding to samples variably carbonated.

The content of fluoride ions was determined by ionometry, using a specific fluoride electrode and Ag/AgCl reference electrode. The determination of fluoride ions is performed in a medium buffered at pH 5.5. The latter is obtained using a complexion solution of trisodium citrate. The results are reported on Table 2.

Phosphate amounts were determined by colorimetry, according to the method of Gee and Deitz [19]. The optical density is measured at $\lambda = 460$ nm (analytical error ±0.2% Table 2).

Determination of calcium amount was performed by complexometry with the tetraacetic ethylene diamine (EDTA) in the presence black erichrome-T. The calcium content is obtained with an analytical error ±0.8% (Table 2).

The density of the solids was determined by the flotation method [6], which consists in determining picnometrically the density of a liquid solution having the same density as the solid. The liquid solution was prepared by mixing diiodomethane ($\rho = 3.315$ g cm^{-3}) and chloroform ($\rho = 1.478$ g cm^{-3}) so as a compact fragment of the solid remains suspended in the bulk of the liquid [20] (Table 2). The experimental molar mass reported in the table was calculated from density measurements and lattice volume determined diffractometrically.

So considering the percentage of calcium, carbonate, fluoride, and phosphate determined by chemical analysis, and the following general chemical formula

$$Ca_\alpha(PO_4)_{(6-x)}(CO_3)_xF_\beta.$$

with $\alpha = 10 - x + u$ the number of calcium ions, x the number of carbonate ions and $\beta = 2 - x + 2u$ the number of fluoride ions in the unit cell of the apatite, one can derive the molar mass as:

$$M = 40\alpha + 35x + 19\beta + 570 \text{ and the electroneutrality}$$

$$2\alpha = 18 - x + \beta.$$

The number of Ca^{2+}, CO_3^{2-}, PO_4^{3-}, and F^- ions in the unit cell of the apatite and the chemical formula of each synthesized sample are reported in Table 3. This table shows also the calculated molar masses of the compounds. One can notice that these quantities are 2.5% higher than the previously determined ones in only two cases.

Table 2 Contents of ions contained in carbonate fluorapatites

$[CO_3^{2-}]/[PO_4^{3-}]$	0.5	1	2	3	4	5	6
% in mass of CO_3^{2-}/Thermogravimetry	1.58	3.10	3.05	4.17	5.97	7.40	7.45
% in mass of F^-	3.82	3.46	4.13	3.86	4.36	4.45	4.36
% in mass of PO_4^{3-}	50.91	50.50	48.50	47.90	43.942	42.30	41.62
% in mass of Ca^{2+}	38.96	38.95	38.85	37.91	38.91	38.42	38.44
Molar mass experimental	979	975	954	947	941	938	939

Thermochemical study

Dissolution of the solid was performed in a C-80 SETARAM microcalorimeter using the reversal cells. The volume of the phosphoric acid solution (19% w/w P_2O_5) is 4.5 mL and the mass of dissolved solid is in the range 10–180 mg. The lower compartment of the reaction cell is provided with the solid and is tightly isolated from the liquid solution by a metallic cover. After one night stabilization time, the reactants were mixed using the reversing mechanism which allows the calorimeter jacket to be alternatively in the reversal then the direct position.

Dissolution of increasing amounts of solid in the same solution volume was carried out at 25 °C and the recorded signal was processed according to Brahim et al. procedure [21, 22] in order to get the deconvoluted curve. Depending on the solid mass dissolved and the concentration of the solution, this curve presents one, two, or even four peaks and the drawing of the heat energy by integrating the rough signal as a function of the mass of solid dissolved shows two or three segments, each one corresponding to a mass domain in which a particular phenomenon occurs (Figs. 4, 5).

Domain1

This domain lies till m near 40 mg for the least carbonated apatite and till m near 60 mg for the moderately carbonated apatite. No precipitate was observed at the end of the reaction. So this domain corresponds to only dissolution of the solid. Because of the presence of carbonate [23, 24], dissolution leads to more acidic solution, and so the more carbonated the solid, the larger the dissolution domain. Dissolution of more carbonated apatites (5.97 and 7.40% carbonate) showed only one domain on the curve representing the heat energy evolved over the solid mass (not represented curves).

Thermogenesis curves in this domain present a single peak for all the amounts of carbonated apatites (Fig. 6) suggesting the occurrence of a one step dissolution process.

In this domain, the pH of the attack solution is around 0.6 and does not undergo a significant variation after dissolution. Taking into account the distribution diagram of phosphate entities, only H_3PO_4 and $H_2PO_4^-$ can exist in solution, and so dissolution can be schematised as:

$$\begin{aligned}&\left[Ca_{(10-x+u)}(PO_4)_{(6-x)}(CO_3)_xF_{(2-x+2u)}\right]_{(sd)}\\&\quad+(14-x+2u)[H_3PO_4]_{(aq)}\rightarrow(10-x+u)\left[Ca^{2+}\right]_{(aq)}\\&\quad+(2-x+2u)[F^-]_{(aq)}+x[H_2O,CO_2]_{(aq)}\\&\quad+(18-x)\left[H_2PO_4^-\right]_{(aq)}+(2-x+2u)[H_3PO_4]_{(aq)}\end{aligned}$$

with $0 \le x \le 2$ and $u \le x/2$.

From the slope of the curves obtained in this domain, one can deduce the molar enthalpies of dissolution. The values are reported in the Table 4.

Domain2

This domain has been observed for 40 mg $< m <$ 70 mg for low carbonated B–CO_3–Fap (1.58%) (Fig. 4) and for masses >56 mg (Fig. 5) for moderately carbonated apatite (3.05%). In addition, the thermogenesis curve in this domain calculated for various amounts of solids present

Table 3 Mole number of ions and chemical formulae of each synthesized samples

% in mass of CO_3^{2-}	$^{n}Ca^{2+}$	$^{n}PO_4^{3-}$	$^{n}CO_3^{2-}$	$^{n}F^-$	M_{th}	Chemical formulae
1.58	9.88	5.73	0.27	2.03	994	$Ca_{9.88}(PO_4)_{5.73}(CO_3)_{0.27}F_{2.03}$
3.10	9.65	5.50	0.50	1.80	973	$Ca_{9.65}(PO_4)_{5.50}(CO_3)_{0.50}F_{1.80}$
3.05	9.84	5.49	0.51	2.20	988	$Ca_{9.84}(PO_4)_{5.49}(CO_3)_{0.51}F_{2.20}$
4.17	9.83	5.28	0.72	2.37	983	$Ca_{9.83}(PO_4)_{5.28}(CO_3)_{0.72}F_{2.37}$
5.97	9.65	5.02	0.98	2.27	965	$Ca_{9.65}(PO_4)_{5.02}(CO_3)_{0.98}F_{2.27}$
7.40	9.55	4.78	1.22	1.32	921	$Ca_{9.15}(PO_4)_{4.80}(CO_3)_{1.20}F_{1.44}$
7.45	9.52	4.77	1.23	2.26	951	$Ca_{9.52}(PO_4)_{4.77}(CO_3)_{1.23}F_{2.26}$

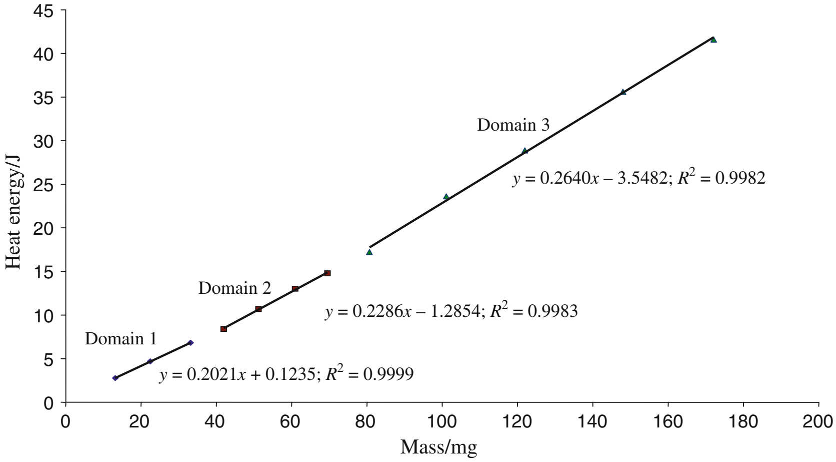

Fig. 4 Heat energy versus the mass of the “B” type carbonate fluorapatite (1.58% carbonate) at 25 °C

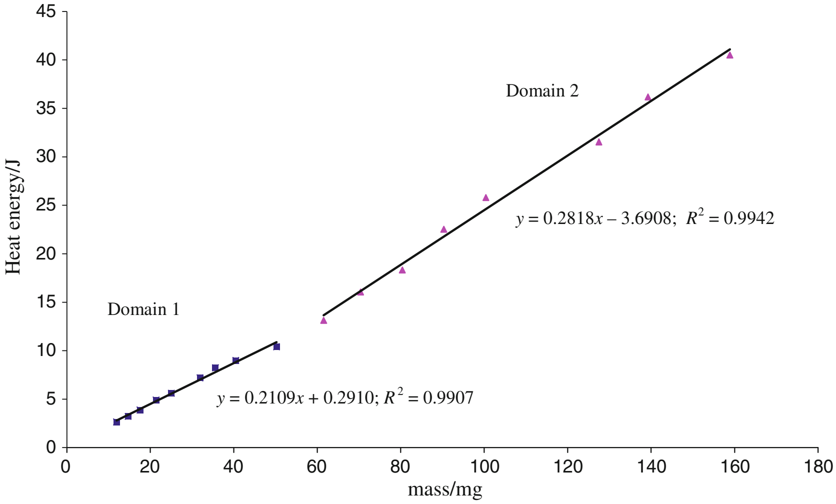

Fig. 5 Heat energy versus the mass of the “B” type carbonate fluorapatite (3.05% carbonate) at 25 °C

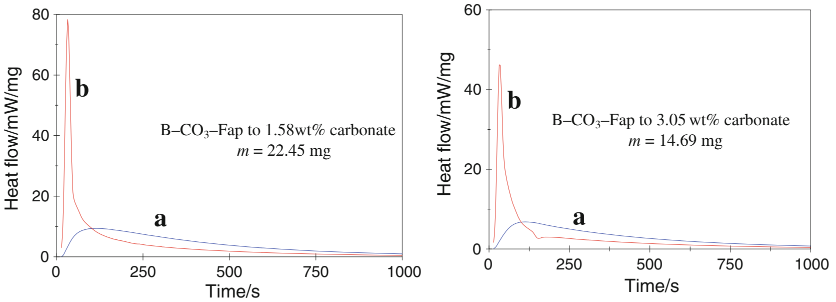

Fig. 6 Heat flow raw (*a*) and thermogenesis (*b*) curves corresponding to the dissolution of 1.58 and 3.05% B–CO_3–Fap in 19% w/w P_2O_5 acid solution at 25 °C

two peaks that overlap for the least carbonated B–CO_3–Fap, three peaks for the moderately carbonated and several peaks for the highly (5.97%) carbonated apatites (Fig. 7).

X-ray analysis of the solids resulting from dissolution in this domain showed CaF_2 for weakly carbonated apatites and a mixture of the latter with $Ca(H_2PO_4)_2{\cdot}H_2O$ for moderately carbonated one, suggesting the occurrence during the attack of two and three steps corresponding to dissolution then precipitation of one or two solids, respectively.

The difference between the slopes of the lines in domains “1” and “2” leads the enthalpy of precipitation of CaF_2 or of the mixture of the latter with $Ca(H_2PO_4)_2{\cdot}H_2O$. That difference equals 0.0265 J mg^{-1} for the least carbonated compound leading to −26.34 kJ per mole CaF_2.

Table 4 Molar enthalpies of dissolution of B–CO_3–Fap apatites

wt% carbonate	1.58%	3.05%
Molar enthalpies/kJ mol^{-1}	−201 ± 4	−208 ± 5

Fig. 7 Heat flow raw (*a*) and thermogenesis (*b*) curves corresponding to the attack of various B–CO_3–Fap by acid solution (19% w/w P_2O_5) at 25 °C

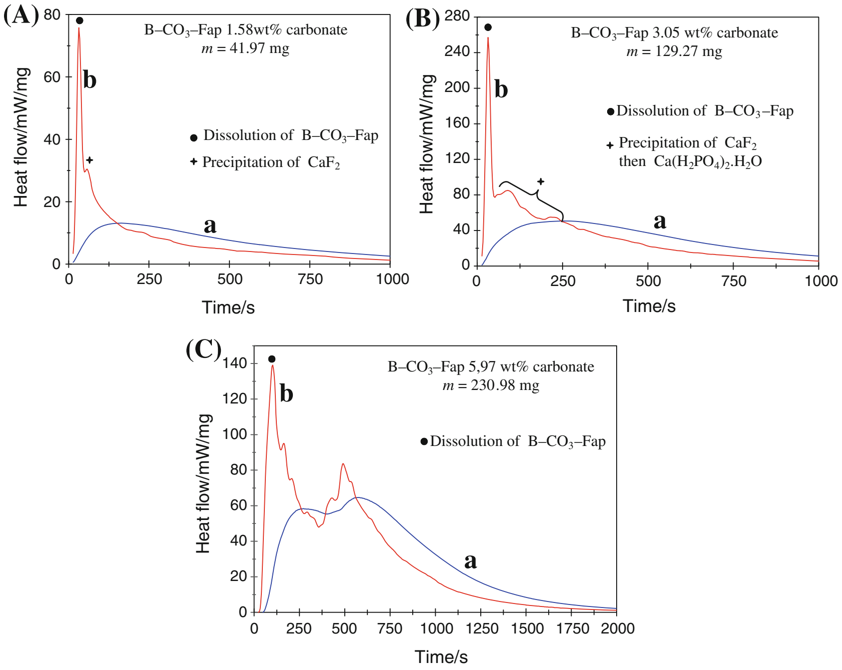

Table 5 Molar enthalpies deduced from the slopes of the lines in domain“2”

wt% carbonate	1.58%	3.05%
Molar enthalpies/kJ mol^{-1}	−228 ± 6	−278 ± 6

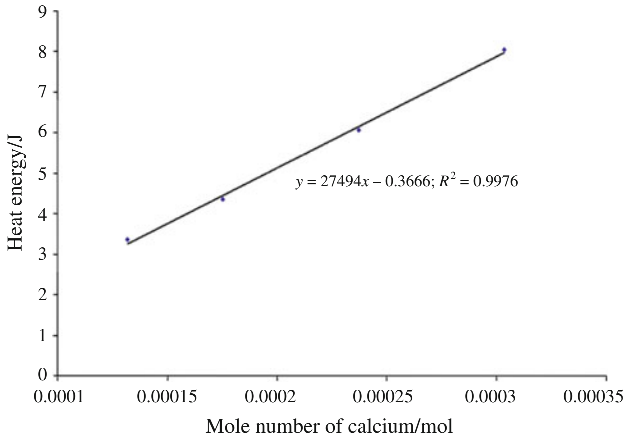

Fig. 8 Graph for determining the enthalpy of precipitation of CaF_2 at 25 °C

The global reaction enthalpies calculated from the slopes of lines in this domain are collected in Table 5.

Enthalpy of precipitation of CaF_2 in conditions close to domain “2” measurements has been determined calorimetrically by mixing a fluoride solution obtained by dissolving ammonium fluoride ($[F^-] = 1.04$ M) in a 19% w/w P_2O_5 solution with a solution containing $CaCO_3$ dissolved in the same acid solution ($[Ca^{2+}] = 0.26$ M).

Various volumes of calcium solution were added to 1 mL of fluoride solution and the plot of the quantity of heat calculated by integrating the raw signal (Q_{mes}) as a function of the mole number of calcium (n^{Ca}_{2+}) allowed to determine the molar enthalpy of precipitation of CaF_2 (Fig. 8). The resulting value is −27.5 ± 0.7 kJ mol^{-1}. This experimental value differs from the previous one by about 4%.

Domain3

This domain has only been observed in the case of the least carbonated B–CO_3–Fap (1.58%), for masses higher than 70 mg (Fig. 4). Thermogenesis curves calculated in this domain present three successive peaks that overlap (Fig. 9). The first peak can be assigned to the dissolution of B–CO_3–Fap, the second one to the formation of calcium fluoride and the third one to the precipitation of monocalcium phosphate monohydrate. These solids have been identified by X-rays diffraction. The overall reaction enthalpy was calculated. From the slope of the straight line segment in domain “3” as −262 ± 10 kJ mol^{-1}.

For the least carbonated apatite the difference between the slopes of the lines in domain “2” and “3” (0.0354 J mg^{-1}) corresponds to the enthalpy of precipitation of $Ca(H_2PO_4)_2{\cdot}H_2O$. Taking into account the molar mass of apatite (994) this leads to −34.8 kJ per mole of $Ca_{9.88}(PO_4)_{5.73}(CO_3)_{0.27}F_{2.03}$ or −3.52 kJ per mole of monocalcium phosphate monohydrate. This value is of the same order of magnitude as that of literature −5.2 kJ mol^{-1} [12].

On the other hand, the differences between the slopes in domain “1” and “2” for moderately carbonate apatites

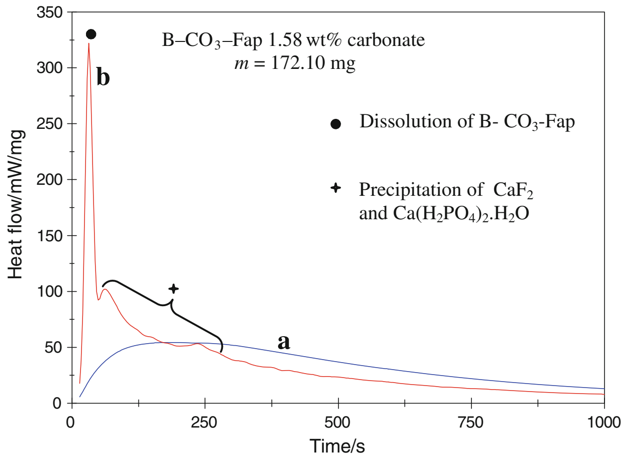

Fig. 9 Heat flow raw (*a*) and thermogenesis (*b*) curves corresponding to the dissolution of 1.58% B–CO_3–Fap in domain "3" at 25 °C

(0.0709 J mg^{-1}) (Fig. 5) corresponds to precipitation of both CaF_2 and $Ca(H_2PO_4)_2 \cdot H_2O$. This value is close to the difference between the slopes in domain "1" and "3" for least carbonated apatite (0.062 J mg^{-1}) (Fig. 4).

As a concluding remark, the incorporation of different amount of carbonate in the B–CO_3–Fap, even at low level seems to lower the molar enthalpy of dissolution. This quantity is around −200 kJ mol^{-1} for the B–CO_3–Fap. The value found by Brahim et al. [11, 12] for noncarbonated Fap dissolved in the same acid solution is −170 kJ mol^{-1}. In addition the presence of the carbonate seems to affect the nature of the precipitate formed after dissolution. For the B–CO_3–Fap, CaF_2 or a mixture the latter with $Ca(H_2PO_4)_2 \cdot H_2O$ was observed, whereas for Fap, no CaF_2 was never observed in the precipitate formed after the attack [11, 12]. This probably results from the presence of fluoride in these carbonate apatites in higher amounts than in noncarbonated Fap.

References

1. Naray-Szabo S. The structure of apatite $(CaF)Ca_4(PO_4)_3$. Z Kristtallogr. 1930;75:387–98.
2. Mehmel M. Uber die struktur das apatite. Z Kristallogr. 1930;75:323–31.
3. El Feki H, Khattech I, Jemal M, Rey C. Décomposition thermique d'hydroxyapatites carbonatées sodées. Thermochim Acta. 1994;237:99–110.
4. Khattech I, Jemal M. Study of the thermal decomposition of carbonated fluorapatites. Thermochim Acta. 1985;95:119–28.
5. Petkova V, Yaneva V. Thermal behavior and phase transformations of nanosized carbonate apatite (Syria). J Therm Anal Calorim. 2010;99:179–89. doi:10.1007/s10973-009-0149-6.
6. Vignoles M. Contribution à l'étude des apatites carbonatées de type B. Thèse de Doctorat d'état, INP Toulouse, 1984.
7. Bonel G, Labarthe JC, Vignoles C. Contribution à l'étude structurale des apatites carbonatées de type B. In: Physicochimie et Cristallographie des Apatites d'intérêt biologique. Colloque, CNRS, Paris; 1975. pp 117–125.
8. Khattech I, Jemal M. Décomposition thermique de fluorapatites carbonatées de type B'inverses'. Thermochim Acta. 1987;118: 267–75.
9. Labarthe C, Bonel G, Montel G. Sur la structure et les propriétés des apatites carbonatées de type B phosphocalciques. Ann Chim Fr. 1973;8:289.
10. Bel Hadj Yahia F, Jemal M. Synthesis, structural analysis and thermochemistry of B type carbonate apatites. Thermochim Acta. 2010;505:22–32.
11. Brahim K, Antar K, Khattech I, Jemal M. Etude thermodynamique et cinétique de l'attaque de la fluorapatites par l'acide phosphorique. Ann Chim Sci Mat. 2006;31(5):611–20.
12. Brahim K. Contribution à l'étude thermodynamique et cinétique de l'attaque phosphorique d'une fluorapatite. Application à un phosphate naturel, Thèse de Doctorat, Université de Tunis El Manar; 2006.
13. I. Khattech, Décomposition thermique d'apatites carbonatées de type B synthétiques : Application aux apatites naturelles. Thèse de 3ème cycle, Université de Tunis El Manar; 1986.
14. Elliott JC. Structure and chemistry of the apatites and other calcium orthophosphates. Amsterdam: Elsevier; 1994.
15. Kandori K, Horigami N, Yasukawa A, Ishikawa T. Texture and formation mechanism of fibrous calcium hydroxyapatite. Particle prepared by decomposition of calcium-EDTA chelates. J Am Ceram Soc. 1997;80:1157.
16. Bonel G. Contribution à l'étude de la carbonatation des apatites. II. Synthèse et étude des propriétés physicochimiques des apatites carbonatées de type B. III. Synthèse et étude des propriétés physico-chimiques d'apatites carbonatées dans deux types de sites. Evolution des spectres infrarouge en fonction de la composition des apatites. Ann Chim Sci Mat. 1972;7:127–44.
17. R.Z. LeGeros, K.H. Vandemaele and J.P. LeGeros, Transformation of calcium carbonates and calcium phosphates to carbonate apatites: possible mechanism for phosphorite formation. In Proceedings of the second International congress on phosphorus compounds, IMPHOS, Boston; 1980. p. 41.
18. V. Petkova, E. Serafimova, N. Petrova, Y. Pelovski, Thermochemistry of triboactivated natural and NH_4-exchanged clinoptilolite mixed with Tunisian apatite, J Therm Anal Calorim. 2010. doi:10.1007/s10973-010-1224-8.
19. Gee A, Deitz VR. Determination of phosphate by spectrophotometry, Ann Chem. 1953;25:1320–1324.
20. Elfeki H. Synthèse et étude de la décomposition thermique d'hydroxy et de fluroaptites carbonatées phosphocalciques sodées. Thesis, Tunis II University, 1990.
21. Brahim K, Khattech I, Dubés JP, Jemal M. Etude cinétique et thermodynamique de la dissolution de la fluorapatites dans l'acide phosphorique. Thermochim Acta. 2005;436:43–50.
22. Antar K, Brahim K, Jemal M. Etude cinétique et thermodynamique de l'attaque d'une fluorapatite par des mélanges d'acides sulfurique et phosphorique à 25 °C. Thermochim Acta. 2006;449:35–41.
23. Pokrovsky OS, Golubev SV, Schott J. Dissolution kinetics of calcite, dolomite and magnesite at 25 °C and 0 to 50 atm pCO_2. Chem Geol. 2005;217:239–55.
24. Abu-Eishah SamirI, Anabtawi MJJ, Isaac SL. Upgrading of carbonaceous phosphate rocks by direct carbonation with CO_2-water solutions. Chem Eng Processing. 2004;43:1085–94.